EBioMedicine 16 (2017) 204–211

Contents lists available at ScienceDirect

EBioMedicine

journal homepage: www.ebiomedicine.com

Research Paper

Human Neutrophil Peptide 1 Limits Hypercholesterolemia-induced Atherosclerosis by Increasing Hepatic LDL Clearance

Nicole Paulin [a,1], Yvonne Döring [a,1], Sander Kooijman [b,c], Xavier Blanchet [a], Joana R. Viola [a,d], Renske de Jong [a,d], Manuela Mandl [a], Jeffrey Hendrikse [a,d], Maximilian Schiener [a], Philipp von Hundelshausen [a], Anja Vogt [e], Christian Weber [a,f], Khalil Bdeir [g], Susanna M. Hofmann [e,h,i], Patrick C.N. Rensen [b,c], Maik Drechsler [a,d,f,1], Oliver Soehnlein [a,d,f,*,1]

[a] Institute for Cardiovascular Prevention (IPEK), LMU Munich, Munich 80336, Germany
[b] Department of Medicine, Division of Endocrinology, Leiden University Medical Center, 2300 RC Leiden, The Netherlands
[c] Einthoven Laboratory for Vascular Medicine, Leiden University Medical Center, 2300 RC Leiden, The Netherlands
[d] Department of Pathology, AMC, 1105 AZ Amsterdam, The Netherlands
[e] Medizinische Klinik und Poliklinik IV, Klinikum der LMU München, Munich 80336, Germany
[f] DZHK, Partner Site Munich Heart Alliance, Munich 80336, Germany
[g] Department of Pathology and Laboratory Medicine, University of Pennsylvania, Philadelphia, PA 19104, USA
[h] Institute for Diabetes and Regeneration, Helmholtz Center Munich, Germany
[i] German Center for Diabetes Research (DZD) München-Neuherberg, Germany

ARTICLE INFO

Article history:
Received 12 May 2016
Received in revised form 5 January 2017
Accepted 5 January 2017
Available online 7 January 2017

Keywords:
Neutrophil
Human neutrophil peptide
LDL receptor
Atherosclerosis
Hypercholesterolemia

ABSTRACT

Increases in plasma LDL-cholesterol have unequivocally been established as a causal risk factor for atherosclerosis. Hence, strategies for lowering of LDL-cholesterol may have immediate therapeutic relevance. Here we study the role of human neutrophil peptide 1 (HNP1) in a mouse model of atherosclerosis and identify its potent atheroprotective effect both upon transgenic overexpression and therapeutic delivery. The effect was found to be due to a reduction of plasma LDL-cholesterol. Mechanistically, HNP1 binds to apolipoproteins enriched in LDL. This interaction facilitates clearance of LDL particles in the liver via LDL receptor. Thus, we here identify a non-redundant mechanism by which HNP1 allows for reduction of LDL-cholesterol, a process that may be therapeutically instructed to lower cardiovascular risk.

1. Introduction

Atherosclerosis represents the most important cause of morbidity and mortality in developed countries. Intrinsically atherosclerotic vascular disease is an inflammatory condition characterized by aberrant lipid metabolism and a maladapted inflammatory response (Libby et al., 2013). Despite the success of lipid-lowering statins, mortality from atherosclerosis-related pathologies remains high and alternative lipid-targeting approaches are being intensely investigated (Rader, 2016). Based on the inverse association of plasma high-density lipoprotein (HDL)-cholesterol levels and cardiovascular events (Assmann et al., 2002) the 'HDL hypothesis' was formulated wherein an increase in HDL-cholesterol would lead to reduction in adverse cardiovascular events. While preclinical studies with HDL infusion, apolipoprotein (Apo) A1 overexpression or inhibition of cholesterylester transfer protein resulted in inhibition or regression of atherosclerosis (Badimon et al., 1990; Tangirala et al., 1999; Kühnast et al., 2015), recent randomized clinical trials using HDL-cholesterol-raising drugs were largely disappointing (AIM-HIGH Investigators et al., 2011; Barter et al., 2007; Schwartz et al., 2012) hence challenging the importance of HDL cholesterol levels in cardiovascular disease. In contrast, clinical trials of low-density lipoprotein (LDL) lowering drugs as well as careful studies of human genetics of LDL-cholesterol and their relationship to cardiovascular risk have unequivocally established LDL as a causal risk factor. Recent strategies to inhibit proprotein convertase subtilisin/kexin type 9 (PCSK9) have corroborated the efficacy of LDL lowering therapies, although neurocognitive side effects, parenteral delivery routes and costs question the long-term feasibility of this approach (Sabatine et al., 2015). Thus, alternative LDL-cholesterol lowering strategies may be beneficial to a large cohort of patients with hypercholesterolemia (Rader, 2016).

While atherosclerosis-related inflammation is thought to be predominantly macrophage-driven, recent evidence points towards the

* Corresponding author at: Institute for Cardiovascular Prevention, Ludwig-Maximilians-University Munich, Pettenkoferstr. 9, 80336 Munich, Germany.
E-mail address: oliver.soehnlein@gmail.com (O. Soehnlein).
[1] Denote equal contribution.

http://dx.doi.org/10.1016/j.ebiom.2017.01.006

importance of neutrophils (Drechsler et al., 2010). These stimulate atherosclerotic lesion formation by releasing the granule protein cathelicidin which paves the way for inflammatory monocytes (Döring et al., 2012). The most abundant neutrophil-derived granule proteins, however, are human neutrophil peptides (HNPs) comprising approximately 5% of total neutrophil protein. HNPs are antimicrobial polypeptides which exert various inflammatory effects when released extracellularly (Choi et al., 2012). As an example, HNPs can stimulate macrophage polarization towards an inflammatory phenotype (Soehnlein et al., 2008) or enhance microvascular permeability (Bdeir et al., 2010). On the other hand, HNPs are strongly cationic and hence show promiscuous, charge-dependent interactions. In this context heteromers comprised of CCL5 and HNP1 were recently shown to strongly stimulate recruitment of classical monocytes (Alard et al., 2015). In addition, HNP1 was shown to interact with Lp(a) (Bdeir et al., 1999) but the pathophysiological relevance of such interaction remains unclear. Here, we study the role of HNP1 in hypercholesterolemia-induced atherosclerosis and witness its strongly protective effect. HNP1-dependent atheroprotection related to enhanced hepatic clearance of HNP1-LDL complexes, a mechanism that could be therapeutically targeted by repetitive HNP1 delivery.

2. Materials and Methods

2.1. Atherosclerosis Studies

HNP1$^{tg/tg}$ mice (Bdeir et al., 2010) were intercrossed with *Apoe*$^{-/-}$ mice to generate double mutant mice. All genetically modified animals were backcrossed to C57Bl/6 background for at least 10 generations. Female mice were fed a high-fat diet (HFD) (21% fat and 0.15% cholesterol, ssniff) for four weeks to induce early atherosclerotic lesions. In a separate set of experiments, female *Apoe*$^{-/-}$ mice (from The Jackson Laboratory) were treated with HNP1 (10 μg, i.v., every other day, Bachem) or vehicle (PBS, i.v.) during the last four weeks of an eight week period of HFD feeding. While mice in Fig. 1 were obtained from our own breeding facility, mice in Fig. 2 were obtained from a commercial breeder which may explain the differences in atherosclerotic lesion sizes after 4 weeks of HFD feeding.

2.2. Histology, Immunohistochemistry, and Immunofluorescence

The extent of atherosclerosis was assessed in aortic roots by HE staining, lipid depositions were assessed following Oil Red O staining. To define neutrophil and monocyte/macrophage numbers in atherosclerotic plaques, frozen sections of aortic roots were stained with antibodies to Ly6G (1A8, BD Biosciences) and Mac2 (Cedarlane) with a 1:100 dilution. After incubation with a secondary antibody for 30 min at room temperature, sections were analyzed. Nuclei were counterstained by 4′,6-Diamidino-2-phenylindol (DAPI). Liver sections from mice treated with Dil-LDL (Purified human LDL labelled with DiI (1,1′-dioctadecyl- 3,3,3′,3′-tetramethylindocarbocyanine perchlorate), Kalen) in presence or absence of HNP1 were stained with anti-LDLR (Abcam, EP1553Y). A Leica DM4000 microscope with a 25/×0.95 water emersion objective (Leica Microsystems) and a Leica DFC 365FX camera were used to capture images. Leica Qwin Imaging software (Leica Ltd.) was employed for image analysis.

2.3. Lipid Fractionation

For lipoprotein separation, samples from 10 animals per group were pooled (0.25 ml) and subjected to fast performance liquid chromatography (FPLC) gel filtration on two Superose 6 columns connected in series as described previously (Hofmann et al., 2008).

2.4. Flow Cytometry

Blood leukocyte counts were quantified by flow cytometry. Staining of single cell suspensions of blood was conducted using combinations of

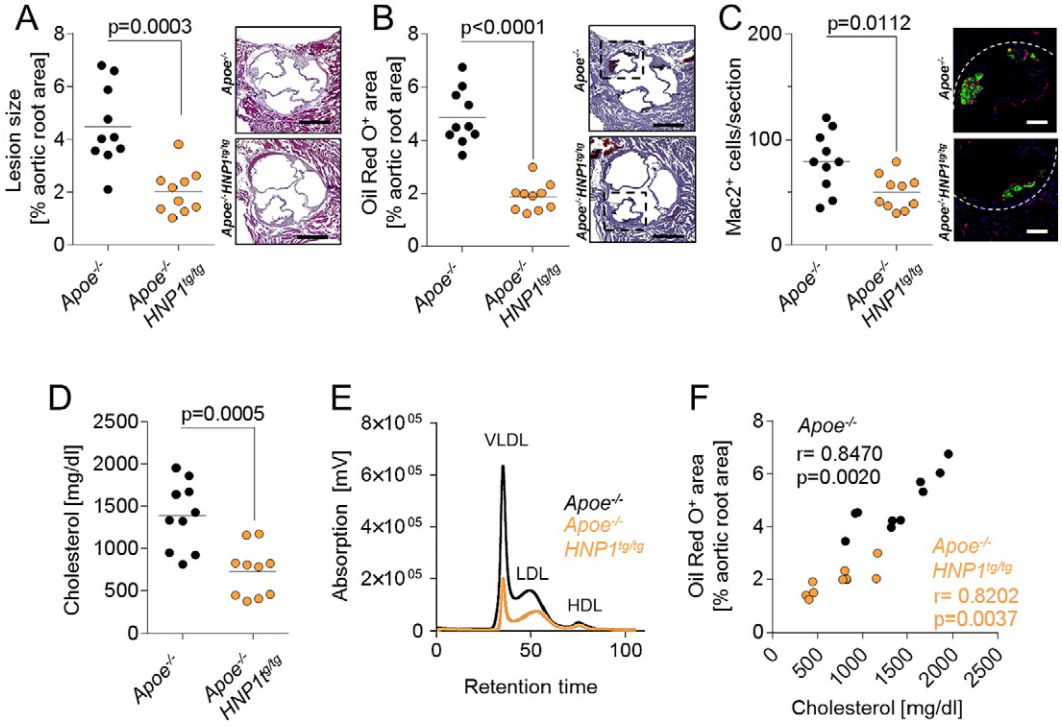

Fig. 1. Transgenic expression of HNP1 protects from atherosclerosis. *Apoe*$^{-/-}$ and *Apoe*$^{-/-}$*HNP1*$^{tg/tg}$ mice were fed a high-fat diet for 4 weeks. (A) Quantification of atherosclerotic lesion sizes in HE-stained aortic root sections. (B) Assessment of lipid deposition in in Oil Red O-stained aortic root sections. (C) Analysis of Mac2^{+} cells indicating macrophage accumulation. Fluorescence images represent macrophages. Valves are zoomed in as indicated by dashed boxes in panel (B). (D) Plasma cholesterol levels. (E) FPLC-assisted fractionation of plasma lipids. (F) Pearson correlation of plasma cholesterol levels and lipid deposition (Oil Red O^{+} area) in aortic root sections. Data in A–D were analyzed by unpaired *t*-test. Scale bars represent 500 μm (A, B) or 100 μm (C).

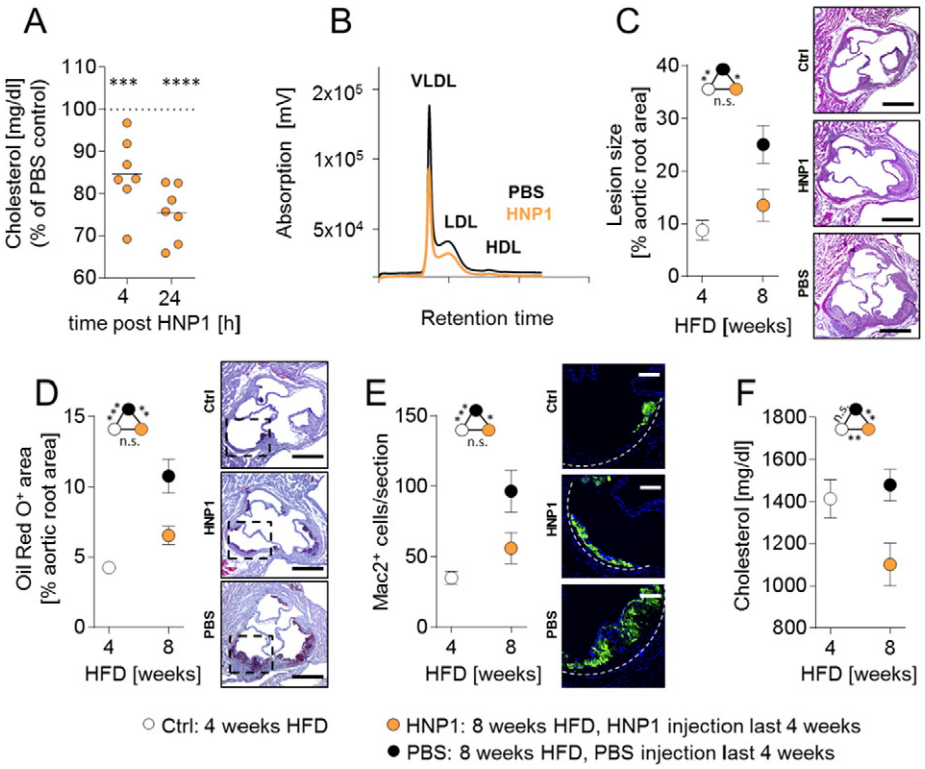

Fig. 2. Treatment with HNP1 reduces hypercholesterolemia-induced atherosclerosis. (A/B) *Apoe*$^{-/-}$ mice were fed a high fat diet for four weeks. Mice were injected with a single dose of HNP1 (10 μg, i.v.) or vehicle (PBS) and plasma was collected after 4 or 24 h. (A) Quantification of plasma cholesterol levels 4 or 24 h after HNP1 or PBS injection. For each time point values obtained from PBS-treated mice were set to 100%. One way-ANOVA. ***$p < 0.001$, ****$p < 0.0001$ vs PBS-treated mice according to Bonferroni multiple comparison test. (B) FPLC-assisted fractionation of plasma lipids 24 h after administration of PBS or HNP1. (C–F) *Apoe*$^{-/-}$ mice were fed a high fat diet for four weeks after which the samples of the baseline group were collected. Two additional groups received either PBS (every other day) or HNP1 (10 μg, every other day, i.v.) during another four weeks of high fat diet feeding. (C) Quantification of atherosclerotic lesion sizes in HE-stained aortic root sections. (D) Quantification of lipid deposition in in Oil Red O-stained aortic root sections. (E) Quantification of Mac2^{+} cells indicating macrophage accumulation. Fluorescence images represent macrophages. Valves are zoomed in as indicated by dashed boxes in panel (D). (F) Plasma cholesterol levels. Data in C–F are presented as mean ± SEM and were analyzed by one-way ANOVA. n = 8–11 per group.*$p < 0.05$, **$p < 0.01$, ***$p < 0.001$ according to Bonferroni multiple comparison test, n.s. not significant. Scale bars represent 500 μm (C, D) or 100 μm (E).

antibodies specific for CD115-PE (eBioscience, AFS98), CD11b-PerCP (BD, M1/70), CD45-APC-Cy7 (BD, 30-F11), and Gr1-APC (eBioscience/BD, RB6-8C5). Before cell staining, red blood cell lysis was performed using appropriate volume of lysis buffer (150 mM NH_4Cl; 10 mM $KHCO_3$; 0.1 mM diNaEDTA, pH 7.4). Cells were washed with Hanks Balanced Salt Solution (HBSS) and directly analyzed by flow cytometry using a FACSCantoII (BD). Absolute cell numbers were assessed by use of CountBright™ absolute counting beads (Invitrogen). Data were analyzed with FlowJo Software (Tree Star Inc.).

2.5. Surface Plasmon Resonance

Surface plasmon resonance was performed on a BIAcore X100 instrument (GE Healthcare) using a CM3 chip. HNP-1 was immobilized using amine-coupling chemistry. The surface of the flow cells were activated for 7 min with a mixture of 0.1 M NHS/EDC at a flow rate of 10 μl/min. The ligand at a concentration of 30 μg/ml in 20 mM sodium acetate, pH 5.0, was immobilized at a density of 260 RU on flow cell 2; flow cell 1 was left blank to serve as a reference surface. The surface was blocked with a 7 min injection of 1 M ethanolamine, pH 8.0. For kinetic analysis, varying concentrations of analytes (62.5 to 1000 ng/ml; human ApoC3, RPB890Hu01, human ApoB, RPC003Hu01, lipid-free, both Cloud-Clone Comp.) were perfused over the chip for 1 min at 90 μl/min in HBS-EP^{+} running buffer (10 mM HEPES, 150 mm NaCl, 3 mm EDTA, 0.05% Surfactant P20, pH 7.4), followed by 20 min of dissociation. Surfaces were regenerated after each injection with two 1 min-pulses of regeneration buffer followed by a 3 min stabilization phase. Sensorgrams were normalized from the baseline signal and kinetic constants were determined using a 1:1 L interaction model available within BIACORE X100 evaluation 2.0 software (GE Healthcare).

2.6. Dot Blot

For dot blot assays, 1 l of mouse plasma was spotted onto a nitrocellulose membrane (0.2 m pore size). Non-specific sites were blocked by soaking in 1% non-fat dry milk in PBS (0.5–1.0 h, RT). The membrane was incubated overnight at 4 °C with respective primary antibody (anti-HNP1, anti-ApoA, anti-ApoB, anti ApoC3, 1:5000, all Abcam) in PBS supplemented with Roti® Block Solution. The membrane was washed with PBS supplemented with 0.05% Tween® 20 and then incubated with diluted horseradish peroxidase (HRP)-linked secondary antibody (1:5000 dilution; Cell Signaling Technology) in PBS supplemented with Roti® Block Solution for 1 h at room temperature, followed by three additional washes in PBS/Tween for 15 min each (3 × 15 min). For analysis, membranes were incubated with ECL substrate and chemiluminescence was recorded (ChemiDoc™ MP System).

2.7. Depletion of Mouse Plasma HNP

HNP were depleted from mouse plasma using anti-HNP conjugated magnetic beads. Briefly, anti-HNP monoclonal antibody (100 μg; ab122884, Abcam) was mixed with Dynabeads® M-270 (3.3×10^8 beads; Invitrogen) in presence of 1 M ammonium sulfate and incubated overnight at room temperature. The coated beads were washed and re-suspended at 2×10^9 beads/ml and added to 50 μl of mouse plasma. The sample was incubated with rotation overnight at room temperature.

Finally, the beads were removed and the depletion was confirmed by dot blot analysis.

2.8. Liver Perfusion Studies

C57BL/6 wild-type or *Ldlr*$^{-/-}$ mice were anesthetized and the abdomen was opened by a mid-line laparotomy. The vena cava was prepared and double ligated. The portal vein was cannulated with a catheter and the liver was perfused with Dil-LDL (50 μg/ml) with HNP1 (10 μg/ml in PBS) or without HNP1 over 20 min (2 ml/min). The liver was then excised, transferred to a culture dish and the tissue was minced to small pieces. The liver homogenate was filtered through a 100 μm cell strainer (BD Pharmingen, yellow, 100 μm pore size) to remove undigested tissue and the cell suspension was centrifuged at 500 g (Eppendorf) for 5 min. After centrifugation the pellet was resuspended in Percoll-HBSS solution (36%) and centrifuged at 800 g for 20 min. Hepatocytes were collected from the top aqueous phase, washed with HBSS and directly analyzed by flow cytometry using a FACS CantoII (BD). LDL uptake was calculated as fold difference from background fluorescence. Data were analyzed with FlowJo Software (Tree Star Inc.).

2.9. Preparation of Radioactively Labelled LDL

Blood was collected from a healthy volunteer. LDL was isolated from serum by density ultracentrifugation and labelling was performed by incubation with liposomes containing glycerol tri[^{3}H]oleate ([^{3}H]TO) and [^{14}C]cholesteryl oleate ([^{14}C]CO) in the presence of thimerosal for 20 h at 37 °C. Subsequently, labelled LDL was separated from liposomes by density ultracentrifugation.

2.10. In vivo LDL Clearance Assays

Apoe$^{-/-}$ mice were fed a Western-type diet for 4 weeks. Human LDL was pre-incubated (10 min; 37 °C) with HNP1 (10 μg in 10 μl PBS) or vehicle (PBS). Mice were fasted for 4 h (from 9.00 h to 12.00 h) and injected i.v. with the radio-labelled control or HNP1 incubated particles via the tail vein. Blood was taken from the tail vein to determine the serum decay of both radiolabels.

2.11. Lipid Uptake Assay

HepG2 cells were cultured in DMEM containing 10% heat-inactivated FCS in a humidified atmosphere of 5% CO_2 at 37 °C. Human LDL (50 μg/ml, Lee Biosolutions) was pre-incubated (30 min; 37 °C) with HNP1 (1 μg, Bachem) or vehicle (PBS). Cells were then treated with or without LDL (50 μg/ml) for 2 h to analyze lipid content. Relative levels of lipids in treated cells were quantified by eluting the Oil Red O dye (Nath et al., 2015).

2.12. Lrp1 and Ldlr Silencing and Heparan Sulfate Proteoglycan Cleavage

For siRNA-mediated silencing, HepG2 were transfected with 100 nM of SMARTpool ON-TARGETplus *Ldlr* siRNA, 100 nM of SMARTpool ON-TARGETplus *Lrp1* siRNA, or 100 nM of ON-TARGETplus nontargeting pool (all Dharmacon) for 24 h in culture medium, as per the manufacturer's instructions. Verification of *Ldlr* and *Lrp1* knockdown was assessed by qRT-PCR analysis. For cleavage of surface heparin sulfate proteoglycans, HepG2 cells were treated with heparinase I and III (1 U/ml, Sigma) for 1 h at 37 °C. After incubation cells were washed and lipid assay was performed as previously described above.

2.13. RNA Isolation and Quantitative Real-time PCR

Total RNA was isolated using RNA Isolations Kit (Quick-RNATM MicroPrep, Zymo Research) according to the manufacturer's protocol. For mRNA quantification, cDNA was synthesized using SuperScript® III First-Strand Synthesis System for RT-PCR (Invitrogen) following the manufacturer's protocol. Quantitative real-time PCR (qRT-PCR) analysis was performed in duplicates using SYBR®Green™qPCR (SuperMix with Premixed ROX, Invitrogen (11794-200)). The mRNA level was normalized to18 S rRNA as housekeeping gene. Relative gene expression was calculated using the $2^{-\Delta\Delta CT}$ method.

2.14. SAA ELISA

Mouse plasma levels of Serum Amyloid A (SAA) were detected by an ELISA Kit (Life Diagnostics, Inc., Catalog Number: SAA-1) according to manufacturer's instructions.

2.15. Plasma Lipid Analysis

Plasma was separated by centrifugation and stored at −80 °C. Total plasma cholesterol and triglycerides were enzymatically measured using the Cholesterol/Triglyceride Assay Kit (Roche/Hitach) according to the manufacturer's instructions.

2.16. Confocal Microscopy

The presence of Dil-LDL in the liver was visualized by confocal microscopy. Briefly, liver sections from mice perfused with Dil-LDL were fixed with 4% formaldehyde, permeabilized with Triton x-100 and incubated with Phalloidin-iFluor647 (Abcam) which selectively binds to F-actins. Nuclei were stained by 4′,6-Diamidino-2-phenylindol (DAPI). A Leica TCS SP8 3× microscope in confocal mode was utilized to capture images. Optimal imaging was performed using a 100 × 1.4 oil objective with additional optical zoom and hybrid diode detectors. Image acquisition and processing was performed using LasX software (Leica).

2.17. Statistics

All data are expressed as mean ± SEM. Statistical calculations were performed using GraphPad Prism 7 (GraphPad Software Inc.). After calculating for normality by D'Agostino Pearson omnibus test, unpaired Student's *t*-test, one-way ANOVA or nonparametric Mann-Whitney test were used as appropriate. p-Values < 0.05 were considered significant.

3. Results

3.1. Reduction of Cholesterol Levels in HNP1-transgenic Mice Correlates With Atherosclerotic Lesion Sizes

With the absence of HNPs in murine neutrophils (Eisenhauer and Lehrer, 1992) we here employed a recently established transgenic mouse model expressing HNP1 (Bdeir et al., 2010). The *HNP1* gene gives rise to both HNP1 and HNP2, the latter being a result of posttranslational modifications. HNP1 and HNP2 comprise 80% of neutrophil HNPs, while HNP3 is only found in low abundance. Thus, the *HNP1*$^{tg/tg}$ mouse model offers a possibility to study the role of HNPs in mice. To assess the relevance of HNP1 in hypercholesterolemia-associated atherosclerosis, we crossed *HNP1*$^{tg/tg}$ mice with *Apoe*$^{-/-}$ mice and fed *Apoe*$^{-/-}$*HNP1*$^{tg/tg}$ and *Apoe*$^{-/-}$ littermates a cholesterol-containing high fat diet for four weeks. Plasma HNP1 levels in HNP1-transgenic mice were in the range of 0.5 to 1 μg/ml (Fig. S1). Thus the plasma levels achieved in these mice are well in the range of what has been reported for conditions associated with activation of neutrophils (Panyutich et al., 1993; Zhao et al., 2012). Lesion sizes in aortic root cross-sections were significantly smaller in HNP1-transgenic mice as compared to control mice (Fig. 1A). In addition, arterial lipid deposition was diminished in transgenic mice (Fig. 1B). Reduction in lesion sizes was associated with a lower grade of lesional inflammation as evidenced by lower total cell numbers and macrophage counts (Fig. 1C & Fig. S2A). The

number of lesional neutrophils was not affected (Fig. S2B), likely being a result of the low frequency of neutrophils per se. In addition, blood counts of leukocyte subpopulations were comparable between the groups excluding major homeostatic effects (Table S1). Thus, these data are in contrast to what is expected, given the reported pro-inflammatory effects of HNP1 (Soehnlein et al., 2008) and especially the importance of HNP1 in leukocyte recruitment (Alard et al., 2015; Chertov et al., 1996).

Consequently, we assumed that instead of acting on inflammatory pathways, HNP1 may rather act on lipid metabolism. Analysis of plasma lipid levels revealed a clear-cut reduction in plasma cholesterol levels in *Apoe*$^{-/-}$*HNP1*$^{tg/tg}$ mice, while triglyceride levels remained unaffected (Fig. 1D & Fig. S2C). The decrease in total plasma cholesterol levels observed in HNP1-transgenic mice was due to a reduced concentration of circulating VLDL and LDL-cholesterol, while HDL-cholesterol remained unaffected (Fig. 1E). Interestingly, plasma cholesterol levels in both *Apoe*$^{-/-}$*HNP1*$^{tg/tg}$ and *Apoe*$^{-/-}$ mice directly correlated with arterial lipid deposition and lesion sizes (Fig. 1F & Fig. S2D). These data suggest that the reduction of plasma cholesterol levels in *Apoe*$^{-/-}$*HNP1*$^{tg/tg}$ mice is a major determinant of reduced arterial lesion development.

3.2. HNP1 Treatment Impedes Atheroprogression

To test if the assumed cholesterol lowering effect can be exploited in a therapeutic approach, we chose to administer a single dose of HNP1 and assessed the resulting plasma cholesterol concentration. Similar to our observations in *Apoe*$^{-/-}$*HNP1*$^{tg/tg}$ mice, HNP1 injection lowered plasma cholesterol levels in a time- and dose-dependent manner which could be attributed to a reduction in circulating VLDL and LDL-cholesterol, but not HDL-cholesterol (Fig. 2A/B & Fig. S3A). To challenge the therapeutic implication of this finding we administered HNP1 or vehicle control (PBS) in hypercholesterolemic mice during the last four weeks of an 8 week high fat diet period (Fig. 2C–F). Compared to lesions harvested at baseline, i.e. mice fed a high fat diet for 4 weeks, HNP1 treatment prevented lesion progression in terms of lesion size and lesional lipid deposition, while lesion development in vehicle-treated mice progressed as shown by 2.8-fold increase in lesion dimension. Beyond lesion extent, the accumulation of macrophages was affected by HNP1 delivery with lower numbers in HNP1-treated mice when compared to mice receiving PBS (Fig. 2E & Fig. S3B). Finally, HNP1 treatment lowered plasma cholesterol levels below baseline levels, while plasma cholesterol levels of mice receiving PBS were not different from baseline levels. Plasma triglyceride levels and blood leukocyte counts were not affected by HNP1 treatment (Fig. S3C & Table S2). In line with observations made in *Apoe*$^{-/-}$*HNP1*$^{tg/tg}$ and *Apoe*$^{-/-}$ mice, plasma cholesterol levels in mice treated with PBS and HNP1 correlated with lesion dimensions in the aortic root (Fig. S3D) supporting the relevance of plasma cholesterol levels to disease progression in this model. Taken together, we so far established the cholesterol-lowering effect of HNP1 and subsequent experiments aimed at defining the underlying mechanisms.

3.3. HNP1 Forms Complexes With (V)LDL

HNPs are promiscuous molecules intermingling with lipids and peptides, interactions essential for antimicrobial activities and receptor engagement (Alard et al., 2015; Bonucci et al., 2013; Doss et al., 2009). To assess the interaction between HNP1 and plasma lipid components, we spotted lipoprotein fractions of mice treated with HNP1 onto a nitrocellulose membrane and stained with antibodies directed to HNP1 (Fig. 3A). In line with the decrease of VLDL and LDL following HNP1 administration, HNP1 was only detected in VLDL and LDL fractions but not in HDL fractions. In the HNP1-positive fractions ApoB and ApoC3 were detected but not ApoA1, the latter being an HDL-selective apolipoprotein. Thus, these data suggest an interaction between HNP1 lipoprotein fractions that contain ApoB and ApoC3. To study the biophysical interaction between HNP1 and plasma lipoproteins or recombinant apolipoproteins we employed surface plasmon resonance with HNP1 being immobilized as bait ligand (Fig. 3B/C). Perfusion of LDL and HDL revealed a strong interaction between HNP1 and human LDL ($K_D = 1.19 \pm 0.08 \times 10^{-11}$ M), while the interaction with human HDL was found to be markedly weaker ($K_D = 2.48 \pm 0.15 \times 10^{-10}$ M). In line herewith, HNP1 was found to have a high affinity for human ApoC3 ($K_D = 3.58 \pm 0.39 \times 10^{-11}$ M) and human ApoB ($K_D = 2.45 \pm 0.18 \times 10^{-9}$ M) (Fig. S4A/B). To test if this interaction could be held responsible for the LDL-cholesterol depleting effect of HNP1, we mimicked the possible mechanism in vitro (Fig. 3D–F). Herein plasma from hypercholesterolemic mice was incubated with HNP1 and magnetic beads conjugated with antibodies to HNP1. Following precipitation of the beads about 70% of the plasma cholesterol was depleted and found to be bound to the anti-HNP1 coupled beads. In addition, the precipitate stained positive for ApoB and ApoC3 suggesting an interaction between HNP1 and these two lipoproteins. In contrast, absence of HNP1 failed to deplete plasma cholesterol.

3.4. HNP1 Enhances LDL Clearance in the Liver

Since HNP1 may impact on lipid metabolism in several ways including decreased synthesis or enhanced clearance we chose to perform in vivo clearance assays. Herein, we isolated human LDL and labelled the lipids with glycerol tri[^{3}H]oleate ([^{3}H]TO) and [^{14}C]cholesteryl oleate ([^{14}C]CO). Labelled LDL was injected intravenously and the plasma half-life was calculated following repetitive blood drawing. In these experiments preincubation of LDL with HNP1 reduced the half-life of LDL-cholesterol from 93.8 min in absence of HNP1 to 43.8 min in presence of HNP1. This indicated that HNP1 not just binds to LDL but also changes its behavior. Since the liver is the primary organ of LDL clearance, we suspected that HNP1 may stimulate LDL uptake in hepatocytes. Thus, LDL uptake by HepG2 was tested in presence or absence of HNP1. In these experiments HNP1 strongly enhanced LDL uptake (Fig. 4A/B). Clearance of LDL in the liver is facilitated by several pathways including engagement of LDL receptor (LDLR), low density lipoprotein receptor-related protein 1 (LRP1), and heparan sulfate proteoglycans. To assess the individual contribution of these pathways we cleaved proteoglycans on hepatocytes by heparinase and specifically silenced LRP1 or LDLR expression by use of siRNA. While neither heparinase treatment nor silencing of LRP1 mitigated HNP1-facilitated uptake of LDL by HepG2 cells, silencing of LDLR abrogated HNP1-assisted LDL clearance (Fig. 4C–E). To confirm this notion in vivo we cannulated the portal vein of normocholesterolemic mice and injected Dil-LDL in presence or absence of HNP1. In these experiments, HNP1 induced a vast increase of LDL uptake in hepatocytes (Fig. 4C–E). As an interaction between HNP1 and LDLR has previously been suggested (Esmaielbeiki et al., 2012) we further assessed the role of LDLR in HNP1-assisted LDL clearance. Thus, the portal vein of *Ldlr*$^{-/-}$ mice was cannulated and Dil-LDL was perfused. In this mouse strain HNP1 failed to stimulate LDL uptake in the liver indicating the functional relevance of LDLR (Fig. 4D). Importantly, repeated delivery of HNP1 in hypercholesterolemic *Apoe*$^{-/-}$ mice also enhanced LDLR expression in the liver (Fig. S5). Thus, HNP1 may facilitate LDL clearance via LDLR in two complementary pathways.

4. Discussion

Hypercholesterolemia is a primary risk factor for the development of atherosclerotic lesions. Despite beneficial effects of lipid-lowering statins, mortality from atherosclerosis-associated cardiovascular diseases remains high. We here investigated the importance of HNP1 in the context of atherosclerosis. With the lack of HNP1 in mice we employed a strategy of transgenic HNP1 expression and find that these mice have lower VLDL and LDL following feeding a high fat diet and thus smaller atherosclerotic lesions. Repeated delivery of HNP1 lowers plasma cholesterol levels and slows down progression of

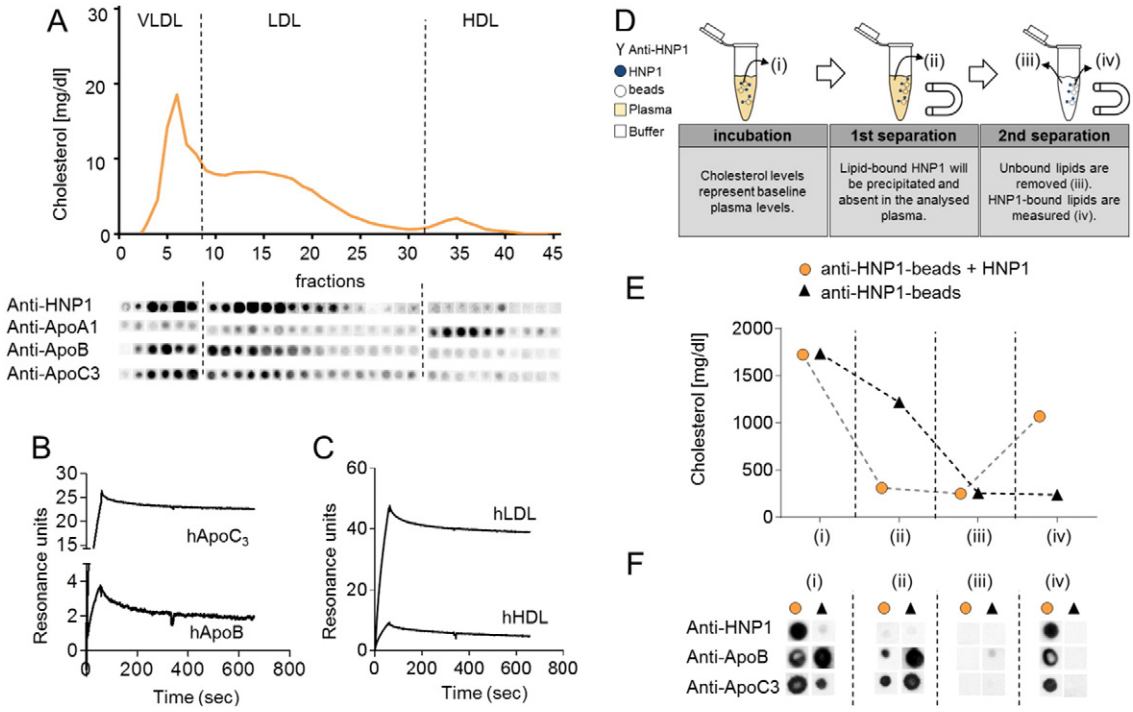

Fig. 3. HNP1 interacts with lipoproteins enriched in VLDL and LDL with high affinity. (A) *Apoe*$^{-/-}$ mice were fed a high fat diet and injected with HNP1 (10 μg, i.v.) and plasma was collected after 24 h. FPLC-assisted fractionation of plasma lipids is displayed (top). Lipid fractions of HNP1-treated mice were spotted on a nitrocellulose membrane and probed with antibodies to HNP1, ApoA1, ApoB, and ApoC3 (bottom). (B/C) Surface plasmon resonance reveals interaction between HNP1 and human apolipoproteins ApoC3 or ApoB (B) or human plasma lipoproteins (hLDL or hHDL) (C). Indicated apolipoproteins or plasma lipoproteins were perfused over a biacore sensor chip coated with HNP1 and the resulting response was assessed. (D–F) Precipitation of lipid-bound HNP1 reduces plasma cholesterol levels. Experimental outline is detailed in (D). Please note the definition of samples (i), (ii), (iii), (iv). Cholesterol levels obtained at different steps (i), (ii), (iii), and (iv) of precipitation (E). Precipitated samples were spotted onto a nitrocellulose membrane and probed with indicated antibodies (F).

existing atherosclerotic lesions. Mechanistically, HNP1 binds to apolipoproteins enriched within VLDL and LDL and consequently accelerates LDL clearance by hepatocytes in a process involving LDLR (Fig. S6). Of note, elevated plasma levels of HNP1 were previously shown to correlate with lower levels of plasma cholesterol and LDL in patients thus indicating that the observations made here may indeed be relevant to

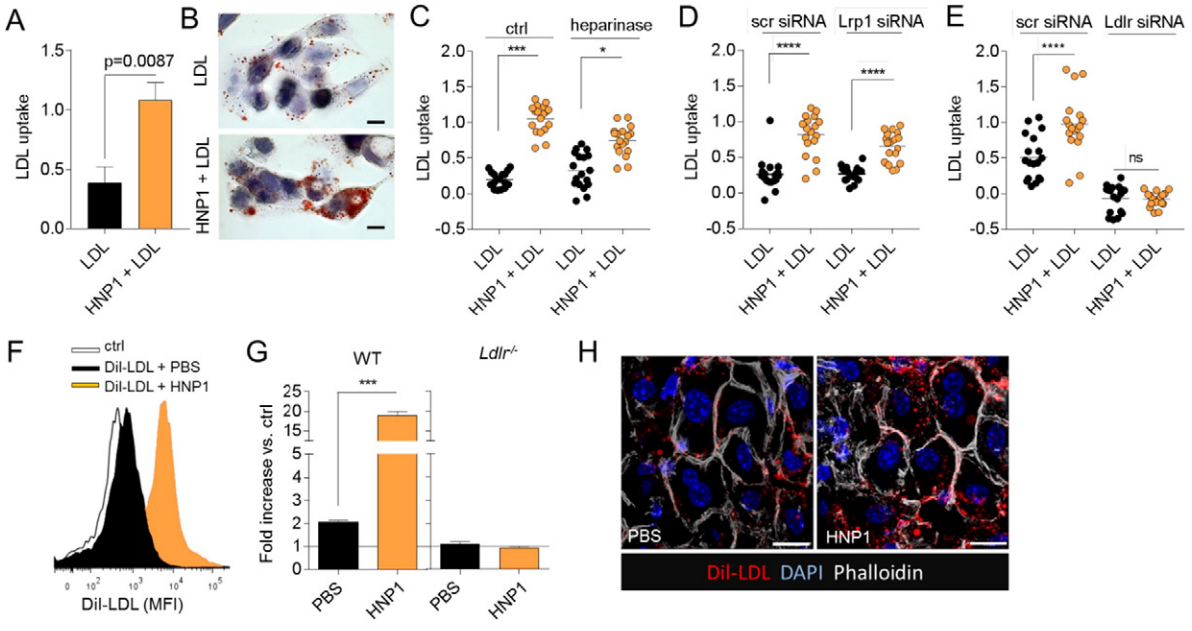

Fig. 4. HNP1 employs LDLR to shuttle LDL into the liver. (A–E) Uptake of human LDL by HepG2 cells. (A/B) HepG2 cells were treated with human LDL (50 μg/ml) in presence or absence of HNP1 (1 μg/ml) for 2 h and LDL uptake was quantified following Oil Red O elution. Representative images for Oil Red O staining are shown in (B). 40× magnification. (C) HepG2 cells were treated with heparinase I and III (1 U/ml, 1 h) or vehicle prior to exposure to LDL. (D/E) *Lrp1* (D) or *Ldlr* (E) were silenced by use of siRNA prior to LDL treatment. (F–H) The portal vein of wild type (WT) or *Ldlr*$^{-/-}$ mice was cannulated and perfused with human Dil-LDL preincubated with HNP1 (10 μg/ml) or PBS. Livers were minced and analyzed by flow cytometry. (F) Representative histograms of Dil-LDL fluorescence in WT mice. (G) Quantification of Dil-LDL uptake relative to background fluorescence (ctrl) which was set to 1. n = 3 per group, data were analyzed by Mann-Whitney test. (H) Confocal microscopy of liver sections from WT mice perfused with Dil-LDL preincubated with PBS or HNP1. Scale bar represents 10 μm.

human pathophysiology (López-Bermejo et al., 2007). These findings contribute to the understanding of LDL uptake in the liver and possibly serve as basis for a strategy to therapeutically lower hypercholesterolemia in patients with cardiovascular risk.

Hypercholesterolemia primes circulating neutrophils, a process associated with enhanced intracellular formation of reactive oxygen species, shedding of CD62L, enhanced surface expression of CD11b, and release of granule proteins including myeloperoxidase. It is thought that these processes contribute to heightened neutrophil recruitment and atherosclerotic lesion formation (Soehnlein, 2012). The degree of neutrophil activation and production has been suggested as biomarker and predictor of future cardiovascular events. Myeloperoxidase and HNP1 are located in the same granule subset within neutrophils and hence hypercholesterolemia enhances plasma HNP1 levels. The interaction of HNP1 with LDL has recently been evidenced in human plasma samples (Abu-Fanne et al., 2016). In this study intravenous administration of HNP1-LDL complexes accumulated primarily in the liver and 10-fold less in the wall of large arteries. In accordance with our findings, total cholesterol levels as well as LDL plasma levels were reduced in mice expressing HNP1 although cholesterol levels in this study remained normocholesterolemic. In this specific setting, transgenic expression of HNP1 facilitated the development of very small lipid deposits after prolonged periods of high fat diet feeding possibly due to the retention of HNP1-LDL complexes in the vasculature likely as a consequence of the interaction with endothelial cells and extracellular matrix (Higazi et al., 2000; Bdeir et al., 1999).

In the context of hypercholesterolemia we find that HNP1-mediated LDL lowering is atheroprotective. Clearance of LDL in the liver is mediated by several complementary pathways. LRP1 (also known as the ApoE receptor or α2-macroglobulin receptor) is expressed on hepatocytes and is known to be involved in diverse activities that include lipoprotein transport. >40 ligands have been reported among these ApoE and HNP1. However, the interaction of HNP1 with LRP1 may be of relevance during the HNP1 assisted monocyte adhesion and activation of smooth muscle cells (Quinn et al., 2011; Nassar et al., 2002) but appears without contribution during HNP1-facilitated LDL uptake in HepG2 cells. Heparan sulfate proteoglycans are abundantly expressed on the surface of hepatocytes and contribute to the clearance of atherogenic lipids. Interestingly, HNP1 interacts with proteoglycans on endothelial cell surface and in this setting enhances endothelial retention of LDL (Higazi et al., 2000). Finally, LDLR receptor recognizing ApoB and ApoE promotes hepatic uptake of LDL. Silencing of LDLR on hepatocytes and the use of *Ldlr*$^{-/-}$ mice in the here presented study points towards the importance of LDLR in HNP1-assisted hepatic LDL uptake. Several mechanisms including the recruitment of a co-receptor or the exposure of neoepitopes on ApoB to enhance association via the LDLR can be envisioned and require further studies. In addition, it is a limitation of the here presented study that observations are restricted to *Apoe*$^{-/-}$ mice. The lipid profile in these mice is discordant from human patients with hypercholesterolemia and hence additional studies in species with a human-like lipid profile are warranted to validate our findings. Finally, while much of the here presented data speak in favor of enhanced LDL cholesterol clearance in the liver, repeated administration of HNP1 may impact on the composition of the gut microbiome and hence intestinal lipid uptake.

HNP1 is the most abundant granule protein in neutrophils. While neutrophils have previously been found to be pro-atherogenic by instructing monocyte recruitment (Drechsler et al., 2010; Döring et al., 2012), the here presented data may seemingly suggest an opposite effect. However, rather than attributing a role to one cell type per se, it is important to appreciate that a cell type and proteins and lipids released from it may exert ambivalent roles. As an example, living neutrophils are traditionally considered pro-inflammatory due to the release of reactive oxygen species and proinflammatory proteins. However, neutrophils also contribute to the production of resolving lipid mediators at later phases of inflammation (Viola et al., 2016). In addition, dying neutrophils upregulate CCR5 and hence scavenge CCL5 and efferocytosis of apoptotic neutrophils promotes a resolving macrophage phenotype (Ortega-Gomez et al., 2013). Thus, the overall impact of neutrophils may be context dependent and given differences between human and murine neutrophils, conclusions drawn from mouse models will have intrinsic shortcomings. The lack of HNPs in murine neutrophils but also of other proteins such as azurocidin may serve as some examples.

With the important causal contribution of LDL cholesterol to cardiovascular disease, several therapeutic strategies aimed at lowering plasma LDL cholesterol have emerged in recent years. Herein, the cholesterol absorption inhibitor ezetimibe and bile acid sequestrants reduce hepatocyte cholesterol leading to transcriptional upregulation of the LDL receptor. PCSK9 inhibitors prevent degradation of the LDLR and post-translationally increase its presence on the hepatocyte cell surface. In our study we present an alternative mechanism wherein HNP1 opsonizes apolipoproteins enriched in LDL thus facilitating the clearance by the liver via LDLR engagement. Given this non-redundant mode of action, HNP1 may lower plasma LDL cholesterol levels even in patients receiving statins or PCSK9 inhibitors. Such mechanism may not just be of relevance to atherosclerosis but also other pathologies including sepsis and critical care. There, septic patients were shown to have a hypocholesterolemia. Together with higher plasma HNP1 levels under these conditions (Chiarla et al., 2010; Martin et al., 2015) our findings may provide a potential mechanism to connect these two events. Since the degree of hypocholesterolemia under septic conditions correlates with disease prognosis, our findings suggest that interference with HNP1-LDLR interactions may be one way to correct the hypocholesterolemia under these conditions. Of note, in the context of acute inflammatory settings also HDL levels are reduced, a finding we could not recapitulate in HNP1-transgenic mice. Thus, in the complex acute phase response where an extensive pattern of protein changes occurs, likely also other mechanism contribute to hypocholesterolemia and hence additional studies will be required to address the overall importance of HNP1 in lipid lowering in the context of acute inflammation. Interestingly, patients with myelocytic leukemia have lower plasma LDL cholesterol levels, which can be reversed following chemotherapy (Budd and Ginsberg, 1986; Ghalaut et al., 2006). The potential involvement of HNP1 released from myeloid cells in LDL cholesterol lowering in these patients is, however, unknown and will require further experimental assessment. In contrast, in patients with hypercholesterolemia, therapeutic instruction of the HNP1-LDLR axis offers a non-redundant approach to lower plasma LDL levels and may hence be beneficial to large cohorts of patients with high cardiovascular risk. With its antimicrobial activity and its abilities to limit neovascularization and tumor progression (Xu et al., 2008; Economopoulou et al., 2005), potential side effects of HNP1 treatment seem limited but require careful assessment.

Funding Sources

This study was supported from the Else Kröner Fresenius Stiftung (2012_A36), the German Research Foundation (SO876/6-1, SO876/11-1, SFB914 B08, SFB1123 A06, B05, A01), the NWO (VIDI project 91712303), and the FöFoLe program of the medical faculty of the LMU Munich (FöFoLe 775). The authors declare no competing financial interests. PCNR is Established Investigator of the Dutch Heart Foundation (2009T038). The confocal microscopic imaging was supported by grants from the German Research Foundation (INST 409/150-1 FUGG, SFB1123/Z01).

Conflict of Interest

None declared.

Author Contributions

N. P. performed and analyzed experiments and contributed to manuscript writing, Y.D. and M.D. contributed to study design, supervision, data analysis, and funding, S. K., X. B., J. R. V., R. d. J., M. M., J. H., M. S., and S. M. H. contributed to data acquisition, P. v. H., A. V., and C. W. provided infrastructure and intellectual input, K. B. provided mice, P. R. contributed to study design, supervision and manuscript preparation, O. S. designed the study and supervised the project, wrote the manuscript, and provided funding.

Acknowledgements

The authors would like to thank Patricia Lemnitzer, Yvonne Jansen, Janine Brauner, and Sebastian Cucuruz for excellent technical assistance. The graphical abstract was designed by Patrick Paulin (Patrick_Paulin@hotmail.de). We thank Lars König for providing HepG2 cells.

Appendix A. Supplementary Data

Supplementary data to this article can be found online at http://dx.doi.org/10.1016/j.ebiom.2017.01.006.

References

Abu-Fanne, R., Maraga, E., Abd-Elrahman, I., Hankin, A., Blum, G., Abdeen, S., Hijazi, N., Cines, D.B., Higazi, A.A., 2016. α-Defensins induce a post-translational modification of low density lipoprotein (LDL) that promotes atherosclerosis at normal levels of plasma cholesterol. J. Biol. Chem. 291, 2777–2786.

AIM-HIGH Investigators, Boden, W.E., Probstfield, J.L., Anderson, T., Chaitman, B.R., Desvignes-Nickens, P., Koprowicz, K., McBride, R., Teo, K., Weintraub, W., 2011. Niacin in patients with low HDL cholesterol levels receiving intensive statin therapy. N. Engl. J. Med. 365, 2255–2267.

Alard, J.E., Ortega-Gomez, A., Wichapong, K., Bongiovanni, D., Horckmans, M., Megens, R.T., Leoni, G., Ferraro, B., Rossaint, J., Paulin, N., et al., 2015. Recruitment of classical monocytes can be inhibited by disturbing heteromers of neutrophil HNP1 and platelet CCL5. Sci. Transl. Med. 7, 317ra196.

Assmann, G., Cullen, P., Schulte, H., 2002. Simple scoring scheme for calculating the risk of acute coronary events based on the 10-year follow-up of the prospective cardiovascular Münster (PROCAM) study. Circulation 105, 310–315.

Badimon, J.J., Badimon, L., Fuster, V., 1990. Regression of atherosclerotic lesions by high density lipoprotein plasma fraction in the cholesterol-fed rabbit. J. Clin. Invest. 85, 1234–1241.

Barter, P.J., Caulfield, M., Eriksson, M., Grundy, S.M., Kastelein, J.J., Komajda, M., Lopez-Sendon, J., Mosca, L., Tardif, J.C., Waters, D.D., et al., 2007. Effects of torcetrapib in patients at high risk for coronary events. N. Engl. J. Med. 357, 2109–2122.

Bdeir, K., Cane, W., Canziani, G., Chaiken, I., Weisel, J., Koschinsky, M.L., Lawn, R.M., Bannerman, P.G., Sachais, B.S., Kuo, A., et al., 1999. Defensin promotes the binding of lipoprotein(a) to vascular matrix. Blood 94, 2007–2019.

Bdeir, K., Higazi, A.A., Kulikovskaya, I., Christofidou-Solomidou, M., Vinogradov, S.A., Allen, T.C., Idell, S., Linzmeier, R., Ganz, T., Cines, D.B., 2010. Neutrophil alpha-defensins cause lung injury by disrupting the capillary-epithelial barrier. Am. J. Respir. Crit. Care Med. 181, 935–946.

Bonucci, A., Balducci, E., Pistolesi, S., Pogni, R., 2013. The defensin-lipid interaction: insights on the binding states of the human antimicrobial peptide HNP-1 to model bacterial membranes. Biochim. Biophys. Acta 1828, 758–764.

Budd, D., Ginsberg, H., 1986. Hypocholesterolemia and acute myelogenous leukemia. Association between disease activity and plasma low-density lipoprotein cholesterol concentrations. Cancer 58, 1361–1365.

Chertov, O., Michiel, D.F., Xu, L., Wang, J.M., Tani, K., Murphy, W.J., Longo, D.L., Taub, D.D., Oppenheim, J.J., 1996. Identification of defensin-1, defensin-2, and CAP37/azurocidin as T-cell chemoattractant proteins released from interleukin-8-stimulated neutrophils. J. Biol. Chem. 271, 2935–2940.

Chiarla, C., Giovannini, I., Giuliante, F., Zadak, Z., Vellone, M., Ardito, F., Clemente, G., Murazio, M., Nuzzo, G., 2010. Severe hypocholesterolemia in surgical patients, sepsis, and critical illness. J. Crit. Care 25, 361.

Choi, K.Y., Chow, L.N., Mookherjee, N., 2012. Cationic host defence peptides: multifaceted role in immune modulation and inflammation. J. Innate Immun. 4, 361–370.

Döring, Y., Drechsler, M., Wantha, S., Kemmerich, K., Lievens, D., Vijayan, S., Gallo, R.L., Weber, C., Soehnlein, O., 2012. Lack of neutrophil-derived CRAMP reduces atherosclerosis in mice. Circ. Res. 110, 1052–1056.

Doss, M., White, M.R., Tecle, T., Gantz, D., Crouch, E.C., Jung, G., Ruchala, P., Waring, A.J., Lehrer, R.I., Hartshorn, K.L., 2009. Interactions of alpha-, beta-, and theta-defensins with influenza A virus and surfactant protein D. J. Immunol. 182, 7878–7887.

Drechsler, M., Megens, R.T., van Zandvoort, M., Weber, C., Soehnlein, O., 2010. Hyperlipidemia-triggered neutrophilia promotes early atherosclerosis. Circulation 122, 1837–1845.

Economopoulou, M., Bdeir, K., Cines, D.B., Fogt, F., Bdeir, Y., Lubkowski, J., Lu, W., Preissner, K.T., Hammes, H.P., Chavakis, T., 2005. Inhibition of pathologic retinal neovascularization by alpha-defensins. Blood 106, 3831–3838.

Eisenhauer, P.B., Lehrer, R.I., 1992. Mouse neutrophils lack defensins. Infect. Immun. 60, 3446–3447.

Esmaielbeiki, R., Naughton, D.P., Nebel, J.C., 2012. Structure prediction of LDLR-HNP1 complex based on docking enhanced by LDLR binding 3D motif. Protein Pept. Lett. 19, 458–467.

Ghalaut, V.S., Pahwa, M.B., Sunita, Ghalaut, P.S., 2006. Alteration in lipid profile in patients of chronic myeloid leukemia before and after chemotherapy. Clin. Chim. Acta 366, 239–242.

Higazi, A.A., Nassar, T., Ganz, T., Rader, D.J., Udassin, R., Bdeir, K., Hiss, E., Sachais, B.S., Williams, K.J., Leitersdorf, E., Cines, D.B., 2000. The alpha-defensins stimulate proteoglycan-dependent catabolism of low-density lipoprotein by vascular cells: a new class of inflammatory apolipoprotein and a possible contributor to atherogenesis. Blood 96, 1393–1398.

Hofmann, S.M., Perez-Tilve, D., Greer, T.M., Coburn, B.A., Grant, E., Basford, J.E., Tschöp, M.H., Hui, D.Y., 2008. Defective lipid delivery modulates glucose tolerance and metabolic response to diet in apolipoprotein E-deficient mice. Diabetes 57, 5–12.

Kühnast, S., van der Tuin, S.J., van der Hoorn, J.W., van Klinken, J.B., Simic, B., Pieterman, E., Havekes, L.M., Landmesser, U., Lüscher, T.F., Willems van Dijk, K., Rensen, P.C., Jukema, J.W., Princen, H.M., 2015. Anacetrapib reduces progression of atherosclerosis, mainly by reducing non-HDL-cholesterol, improves lesion stability and adds to the beneficial effects of atorvastatin. Eur. Heart J. 36, 39–48.

Libby, P., Lichtman, A.H., Hansson, G.K., 2013. Immune effector mechanisms implicated in atherosclerosis: from mice to humans. Immunity 38, 1092–1104.

López-Bermejo, A., Chico-Julià, B., Castro, A., Recasens, M., Esteve, E., Biarnés, J., Casamitjana, R., Ricart, W., Fernández-Real, J.M., 2007. Alpha defensins 1, 2, and 3: potential roles in dyslipidemia and vascular dysfunction in humans. Arterioscler. Thromb. Vasc. Biol. 27, 1166–1171.

Martin, L., van Meegern, A., Doemming, S., Schuerholz, T., 2015. Antimicrobial peptides in human sepsis. Front. Immunol. 6, 404.

Nassar, T., Akkawi, S., Bar-Shavit, R., Haj-Yehia, A., Bdeir, K., Al-Mehdi, A.B., Tarshis, M., Higazi, A.A., 2002. Human alpha-defensin regulates smooth muscle cell contraction: a role for low-density lipoprotein receptor-related protein/alpha 2-macroglobulin receptor. Blood 100, 4026–4032.

Nath, A., Li, I., Roberts, L.R., Chan, C., 2015. Elevated free fatty acid uptake via CD36 promotes epithelial-mesenchymal transition in hepatocellular carcinoma. Sci. Rep. 5, 14752.

Ortega-Gómez, A., Perretti, M., Soehnlein, O., 2013. Resolution of inflammation: an integrated view. EMBO Mol. Med. 5, 661–674.

Panyutich, A.V., Panyutich, E.A., Krapivin, V.A., Baturevich, E.A., Ganz, T., 1993. Plasma defensin concentrations are elevated in patients with septicemia or bacterial meningitis. J. Lab. Clin. Med. 122, 202–207.

Quinn, K.L., Henriques, M., Tabuchi, A., Han, B., Yang, H., Cheng, W.E., Tole, S., Yu, H., Luo, A., Charbonney, E., Tullis, E., Lazarus, A., Robinson, L.A., Ni, H., Peterson, B.R., Kuebler, W.M., Slutsky, A.S., Zhang, H., 2011. Human neutrophil peptides mediate endothelial-monocyte interaction, foam cell formation, and platelet activation. Arterioscler. Thromb. Vasc. Biol. 31, 2070–2079.

Rader, D.J., 2016. New therapeutic approaches to the treatment of dyslipidemia. Cell Metab. 23, 405–412.

Sabatine, M.S., Giugliano, R.P., Wiviott, S.D., Raal, F.J., Blom, D.J., Robinson, J., Ballantyne, C.M., Somaratne, R., Legg, J., Wasserman, S.M., et al., 2015. Efficacy and safety of evolocumab in reducing lipids and cardiovascular events. N. Engl. J. Med. 372, 1500–1509.

Schwartz, G.G., Olsson, A.G., Abt, M., Ballantyne, C.M., Barter, P.J., Brumm, J., Chaitman, B.R., Holme, I.M., Kallend, D., Leiter, L.A., et al., 2012. Effects of dalcetrapib in patients with a recent acute coronary syndrome. N. Engl. J. Med. 367, 2089–2099.

Soehnlein, O., 2012. Multiple roles for neutrophils in atherosclerosis. Circ. Res. 110, 875–888.

Soehnlein, O., Kai-Larsen, Y., Frithiof, R., Sorensen, O.E., Kenne, E., Scharffetter-Kochanek, K., Eriksson, E.E., Herwald, H., Agerberth, B., Lindbom, L., 2008. Neutrophil primary granule proteins HBP and HNP1-3 boost bacterial phagocytosis by human and murine macrophages. J. Clin. Invest. 118, 3491–3502.

Tangirala, R.K., Tsukamoto, K., Chun, S.H., Usher, D., Puré, E., Rader, D.J., 1999. Regression of atherosclerosis induced by liver-directed gene transfer of apolipoprotein A-I in mice. Circulation 100, 1816–1822.

Viola, J.R., Lemnitzer, P., Jansen, Y., Csaba, G., Winter, C., Neideck, C., Silvestre-Roig, C., Dittmar, G., Döring, Y., Drechsler, M., Weber, C., Zimmer, R., Cenac, N., Soehnlein, O., 2016. Resolving lipid mediators maresin 1 and resolvin D2 prevent atheroprogression in mice. Circ. Res. 119, 1030–1038.

Xu, N., Wang, Y.S., Pan, W.B., Xiao, B., Wen, Y.J., Chen, X.C., Chen, L.J., Deng, H.X., You, J., Kan, B., Fu, A.F., Li, D., Zhao, X., Wei, Y.Q., 2008. Human alpha-defensin-1 inhibits growth of human lung adenocarcinoma xenograft in nude mice. Mol. Cancer Ther. 7, 1588–1597.

Zhao, H., Yan, H., Yamashita, S., Li, W., Liu, C., Chen, Y., Zhou, P., Chi, Y., Wang, S., Zhao, B., Song, L., 2012. Acute ST-segment elevation myocardial infarction is associated with decreased human antimicrobial peptide LL-37 and increased human neutrophil peptide-1 to 3 in plasma. J. Atheroscler. Thromb. 19, 357–368.